The 2.5D MST for sound propagation through arrays of cylinders parallel to the ground

Bart van der Aa & Jens Forssén
Department of Civil and Environmental Engineering, Division of Applied Acoustics, Chalmers University of Technology, SE-41296 Göteborg, Sweden.

Summary
In this work sound propagation through arrays of cylinders oriented parallel to the ground is of interest. The structures are placed in a three-dimensional domain and are insonified by a monopole or incoherent line source. Assuming a cross-sectionally invariant structure one can efficiently obtain the 3D pressure field for such arrangements by post-processing a series of 2D solutions - a technique usually referred to as a 2.5D transform. Since the initiation of the 2.5D transform for outdoor sound propagation it has been successfully applied together with frequency domain methods such as the Boundary Element Method and the Equivalent Sources Method. However, to predict for sound propagation through sonic crystal noise barriers the 2D Multiple Scattering Theory (2D MST) is often used, and has proven to be very efficient. We therefore introduce the 2.5D MST to solve for 3D scattering by clusters of acoustically rigid cylinders. It will be shown that only a few simple substitutions applied to the 2D MST kernel allows us to solve for imaginary wave numbers, which are needed in the 2.5D transform. The proposed method is numerically validated for two basic cases: (i) a point source above rigid ground, and (ii) off-axis scattering by a cylinder in free-field. Both are shown to be in excellent agreement with the respective reference calculations. We further demonstrate some calculation results for sound propagation through graded index sonic crystals, and find that off-axis insonification of these structures shifts the characteristic frequency response upwards, as could be expected. Finally, we also present calculation results for infinite and finite incoherent line sources and display the existence of a spectral smearing effect for both source types.

1. INTRODUCTION

In the recent past the interest in sonic crystals has steadily increased among researchers in various fields dealing with acoustic wave-propagation. One of the main reasons it attracted considerable attention is the fact that these structures can be engineered to specific needs. For instance, researchers of various groups have worked on acoustic cloaking devices [1], acoustic waveguides [2], acoustic lenses [3], and noise barriers [4].

In the models used to predict the response of these structures it is often assumed that the source is a plane or cylindrical wave. When the source-to-structure distance is large a plane-wave source function can be assumed with good accuracy. A cylindrical source function is, however, a better choice when the source is placed in the vicinity of the object. Still, one will implicitly assume that amplitude and phase of the source and scattered field are constant along the invariant axis of the geometry. This is not necessarily an issue if the actual source of interest is well described by a coherent line, but may introduce significant discrepancies between predictions and reality when the actual problem is better described by a (finite) incoherent line source or (off-axis) monopole. A study by M. Heckl showed, among other things, that characteristic propagation phenomena of periodically arranged cylindrical scatterers will shift up in frequency for oblique plane wave incidence [5]. In other words, when off-axis source-receiver positions are of interest a two-dimensional (2D) model may not capture the full complexity of a three-dimensional (3D) problem.

The current analysis of sonic crystals, and in particular for sonic crystal noise barriers, is still mostly done by means of 2D models. The 2D Multiple Scattering Theory (2D MST) is therefore often used, and has proven to be very efficient. Now, with the assumption of a cross-sectionally invariant structure the 3D pressure field can be obtained by post-processing a series of 2D solutions - a technique usually referred to as a 2.5D transform. Since the initiation of the 2.5D transform for outdoor sound propagation by Duhamel [6], it has been successfully applied together with frequency domain methods such as the Bound-

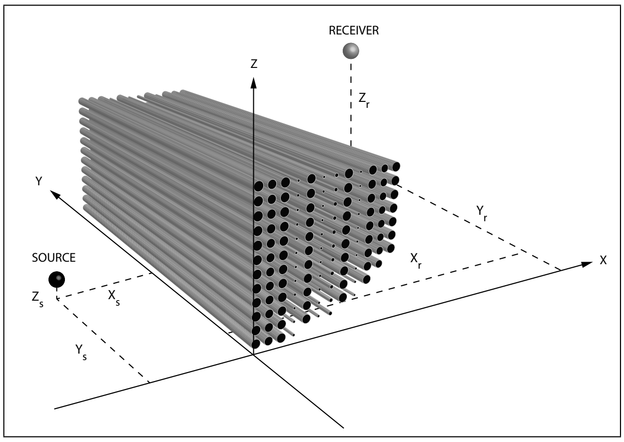

Figure 1. Illustration of a GRIN SC in a three-dimensional domain.

ary Element Method [7, 8] and the Equivalent Sources Method [9]. In the following, we will introduce the 2.5D MST to solve for 3D scattering by clusters of acoustically rigid cylinders parallel to the ground.

The method will be numerically validated for two basic cases: (i) a point source above rigid ground, and (ii) off-axis scattering by a cylinder in free-field. We further demonstrate some calculation results for sound propagation through graded index sonic crystal formations insonified by a monopole source, an infinite incoherent line source, and a finite incoherent line source.

2. THE MODEL

Sound propagation through an array of infinitely long cylindrical scatterers located above rigid ground is considered in a three-dimensional Cartesian space, see Fig 1. A point source and receiver are placed above the ground surface, i.e. $z \geq 0$. In addition, they are assumed to be in the exterior region of the scatterers. The longitudinal axes of the cylinders are placed parallel to the y-axis of the geometry, resulting in an invariant cross-section of the array along the y-direction. As such the problem reduces to a so-called two-and-a-half-dimensional (2.5D) geometry, which can be solved efficiently [6, 7, 8, 9]. Solving a 3D problem in a 2.5D geometry utilising 2D solutions is referred to as a 2.5D method. The crux of this method lies in applying a Fourier transform of the 3D Helmholtz equation with respect to one of the spatial dimensions, here chosen to be the y-direction. What results is essentially a 2D Helmholtz equation as function of an effective wavenumber $K = \sqrt{k^2 - k_y^2}$, in which $k = \sqrt{k_x^2 + k_y^2 + k_z^2}$. The 3D pressure field may then be found by applying an inverse Fourier transform over the wave numbers k_y.

In this work the 2D solutions are obtained using the Multiple Scattering Theory (MST) for cylindrical scatterers, see e.g. [10, 11]. The MST method is a widely used semi-analytical scheme where scattering by a cluster of non-overlapping infinitely long cylindrical scatterers can be formulated efficiently. Classically, the modal scattering terms for cylindrical scattering objects are derived for two-dimensional geometries assuming a cylindrical or plane wave source function. However, these previously derived scattering terms, together with the MST kernel, may also be used to obtain the 3D sound field for monopole excitation in a 2.5D geometry. To do that two main ingredients are needed: (i) the 2.5D transform as initiated in [6], and (ii) the Bessel and Hankel functions used in MST must be substituted with appropriate Modified Bessel functions when $K^2 < 0$, i.e. for imaginary wave numbers. Details about the 2.5D transform and suitable substitutions for MST when $K^2 < 0$ are discussed below.

2.1. The 2.5D transform

Assume a monopole source being located at Cartesian coordinates (x_s, y_s, z_s) and a receiver at (x, y, z). In this work we seek a solution of the Helmholtz equation in three-dimensional space which is given by:

$$\begin{aligned}&\left[\frac{\partial^2}{\partial x^2} + \frac{\partial^2}{\partial y^2} + \frac{\partial^2}{\partial z^2}\right] p + k^2 p \\ &= -4\pi\delta(x - x_s)\delta(y - y_s)\delta(z - z_s),\end{aligned} \quad (1)$$

where, $p(x, y, z)$ is the sound pressure. Applying a Fourier transform of Eq. 1 with respect to the y-direction one arrives at an equation being equivalent to the 2D Helmholtz equation [7, 9]:

$$\left[\frac{\partial^2}{\partial x^2} + \frac{\partial^2}{\partial z^2}\right] q + K^2 q = -4\pi\delta(x - x_s)\delta(z - z_s), \quad (2)$$

where, $K = \sqrt{k^2 - k_y^2}$, and

$$q(x, z, K) = \int_{-\infty}^{\infty} p(x, y, z, k) e^{-ik_y(y_s - y)} dy. \quad (3)$$

The corresponding inverse transform is given by:

$$p(x, y, z, k) = \frac{1}{2\pi} \int_{-\infty}^{\infty} q\left(x, z, K\right) e^{ik_y(y_s - y)} dk_y, \quad (4)$$

and can be approximated by a finite summation series as discussed in e.g. [9]. Note that the summation series as referred to here are based on a modified integral representation of Eq. 4, which consist of four integration domains. For details about the 2.5D transform the reader is referred to e.g. [9].

As reported by several authors, the accuracy of the 2.5D transform is mainly dependent on two factors: (i) the choice of the frequency resolution Δ_f, and (ii) the inclusion of imaginary frequency components in the transform. In brief, $q(x, z, K)$ oscillates as function of k_y, though more rapidly for larger

r_{2D}, where r_{2D} is the source receiver distance in a two-dimensional plane. Hence, to recover these oscillations Δ_f must be chosen smaller for larger r_{2D}. Setting $\Delta_f = c_0/(5r_{2D,max})$, where $r_{2D,max}$ is the maximum distance of interest, typically gives a good accuracy at the oscillations [6]. The role of including imaginary frequency components in the 2.5D transform may be clarified by the point of stationary phase e.g. described by Salomons [7]. The point of stationary phase is found at $k_y = k\sin(\theta)$, with $\theta = \arctan[(y - y_s)/r_{2D}]$, and depicts the region that has the biggest contribution to the integral in Eq. 4. Now, when $r_{2d} \to 0$ or $K \to 0$ the point of stationary phase tends to a singularity, and hence the inclusion of imaginary frequencies becomes increasingly important. This obviously explains the usually poorer performance of the transform for low frequencies and small source to receiver distances.

2.2. The 2.5D MST

As can be concluded from Eq. 4, the 3D pressure for a given k at receiver (x, y, z) can be obtained by integrating with respect to k_y. Here, the integrand is a 2D function multiplied by a phasor, which for multiple scattering by cylinders is straightforward to obtain with MST when $K^2 > 0$. For $K^2 < 0$, the Bessel and Hankel functions used in MST needs special treatment, as will be shown subsequently.

However, we will first briefly introduce the 2D MST for $K^2 > 0$, after which the substitutions for $K^2 < 0$ follows naturally. Let us formulate acoustic scattering by an array of N cylindrical units located above a rigid ground as detailed in e.g. [12]. We assume that a coherent line-source insonifies the array, which is located above the ground surface, i.e. $z \geq 0$. The cylindrical scatterers are acoustically rigid and are organised in square lattice, with a lattice constant a. Each cylinder has an outer radius r_o^j and has been given a local coordinate system $(\hat{r}_j, \hat{\theta}_j)$, where $j = 1, ..., N$. In order to solve for such a configuration, i.e. an array of cylinders above rigid ground, the source and cylinders are mirrored around $z = 0$, which results in $2N$ scattering units and an additional image source. We now have the ingredients to express the total pressure at any point exterior to the scatterers in a series of Hankel and trigonometric functions. When assuming an $e^{-i\omega t}$ time-dependence and $K^2 > 0$ we can write:

$$\begin{aligned} q_o(r, \theta, K) &= H_0(Kr) + H_0(Kr') \\ &+ \sum_{j=1}^{2N} \sum_{n=-\infty}^{\infty} A_n^j Z_n^j H_n(K\hat{r}_j) \exp(in\hat{\theta}_j), \end{aligned} \tag{5}$$

where, $H_n(\cdot)$ is the Hankel function of first kind and order n, and A_n^j are unknown coefficients. The first right-hand term of Eq. 5 is recognised as the source-to-receiver contribution for a source above $z = 0$ m, the second term the source-to-receiver contribution for a source below $z = 0$ m, and the third term the scattered field from all cylinders in the domain. In addition, we introduced the Z_n^j terms to capture the boundary condition of the j-th cylinder which for acoustically rigid cylinders are given by:

$$Z_n^j = \frac{J_n'(Kr_o^j)}{H_n'(Kr_o^j)}. \tag{6}$$

To solve for the unknown A_n^j coefficients in Eq. 5, the equation system must be expressed in one set of polar coordinates $(\hat{r}_j, \hat{\theta}_j)$. This is done by using Graf's addition theorem for Bessel functions applied to Eq. 5. Further, using orthogonality of the terms, and fulfilling the boundary for acoustically rigid surfaces leads to an infinite system of equations:

$$\begin{aligned} & A_m^p + \sum_{\substack{j=1 \\ \neq p}}^{2N} \sum_{n=-\infty}^{\infty} A_n^j Z_n^j e^{i(n-m)\xi_{jp}} H_{n-m}(KR_{jp}) \\ &= -[H_m(KR_p)e^{-im(\pi+\xi_p)} + H_m(KR_p')e^{-im(\pi+\xi_p')}], \end{aligned} \tag{7}$$

$$p = 1, ..., 2N \qquad m = 0, \pm 1, \pm 2, ...$$

where $\mathbf{R_{jp}} = R_{jp}(\cos\xi_{jp}, \sin\xi_{jp})$ is the radius vector from the origin of cylinder j to the origin of cylinder p, $\mathbf{R_p} = R_p(\cos\xi_p, \sin\xi_p)$ is the radius vector from the source above $z = 0$ m to the origin of the p-th cylinder, and $\mathbf{R_p'} = R_p'(\cos\xi_p', \sin\xi_p')$ is the radius vector from the source below $z = 0$ m to the origin of the p-th cylinder. By truncating in both n and m, and rewriting Eq.7 in matrix form allows us to solve for the unknown A_n^j amplitudes. Note that the summation series has been truncated such that $|n|$, $|m| > 3Kr_o$.

The theory as outlined so far is valid for $K^2 > 0$. However, when $K^2 < 0$, an appropriate continuation of the Bessel and Hankel functions used in Eqs. 5 – 7, must be found. Once $\sqrt{k^2 - k_y^2}$ becomes imaginary, the Hankel function should be replaced with the Modified Bessel function according to:

$$H_n(iK) = \frac{2}{\pi i^{n+1}} K_n(K), \tag{8}$$

where, $K_n(K)$ is the Modified Bessel function of second kind and order n. Similarly, the Bessel function of first kind must be replaced by an appropriate continuation, which reads:

$$J_n(iK) = e^{\frac{ni\pi}{2}} I_n(K), \tag{9}$$

where, $I_n(K)$ is the Modified Bessel function of first kind and order n. Note that special attention must be paid to the computation of the Z_n^j terms as the derivatives of the Modified Bessel functions are subjected to sign changes which are different from the ordinary Bessel and Hankel functions.

2.3. Numerical validation cases

At this end we have formulated the tools needed to compute the 3D pressure field for a cross-sectionally invariant array of cylinders above rigid ground. In order to validate the proposed method we will study two basic configurations: (i) a point source above rigid ground, and (ii) off-axis scattering by a cylinder in free field. For the first case we essentially transform the pressure of a cylindrical sound source above rigid ground to a point source above rigid ground. As analytical expressions for both of these source functions exist this seems an appropriate choice to investigate the accuracy of the transform. The second case, i.e. off-axis scattering by a cylinder, will be compared against a 2.5D BEM code which makes use of the same transform routine, but uses a different method to obtain the 2D spectra.

2.3.1. A point source above rigid ground

The solution of Eq. 2 in free-space is known for real and imaginary values of K and has been presented in e.g. [9, 7]. It may also be used to formulate an expression for a cylindrical source above rigid ground which is given by:

$$q(x,z,K) = \begin{cases} i\pi\left[H_0(Kr_{2D,d}) + H_0(Kr_{2D,r})\right] & K^2 \geq 0 \\ 2\left[K_0(|K|\,r_{2D,d}) + K_0(|K|\,r_{2D,r})\right] & K^2 < 0 \end{cases}, \quad (10)$$

where, $r_{2D,d} = \sqrt{(x-x_s)^2 + (z-z_s)^2}$ is the source to receiver distance and $r_{2D,r} = \sqrt{(x-x_s)^2 + (z+z_s)^2}$ is the distance from image source to receiver.

Let us now investigate the error one will introduce by using the 2.5D transform together with $q(x,z,K)$ as specified in Eq. 10. The idea is to compare the transformed spectra against the exact solution of a point source above rigid ground which is given by: $p_{3D} = e^{ikr_{3D,d}}/r_{3D,d} + e^{ikr_{3D,r}}/r_{3D,r}$, in which $r_{3D,r} = \sqrt{r_{2D,r}^2 + (y-y_s)^2}$, and $r_{3D,d} = \sqrt{r_{2D,d}^2 + (y-y_s)^2}$. Assume a source being located at $(x_s, y_s, z_s) = (-2.5, 0, 0.75)$ [m], and two receivers at $(x_r, y_r, z_r) = (10, 0, 1.5)$ and $(50, 100, 1.5)$. We can investigate the accuracy of the transform by setting Δ_f to 1, 0.5 and 0.25 Hz, and compute the error through $E(k) = 20\log\left[|p(x,y,z,k)|\,/\,|p_{3D}(x,y,z,k)|\right]$. Error plots for the configurations as described above are depicted in Fig. 2. It can be seen that the two finest frequency discretisations give a maximum error of about 0.05 dB, whereas the coarsest frequency discretisation showcase a maximum error of about 0.5 dB. Further, we notice the two error maxima at around 1 and 3 kHz in the left panel of Fig. 2. It can be shown that both peaks correspond to ground interference dips, and hence a greater error around those frequencies is expected. In what follows we continue to use a frequency discretisation $\Delta_f = 0.5$ Hz.

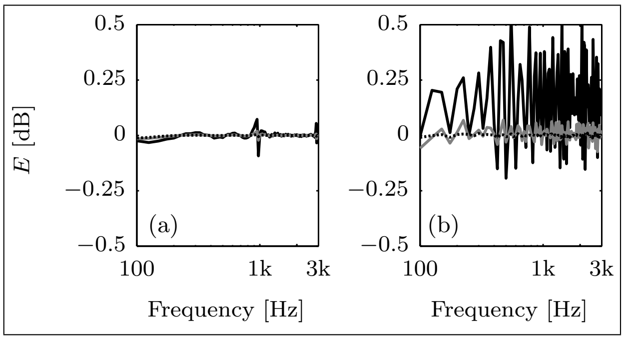

Figure 2. Error in the 2.5D transform for a point source above rigid ground. (a): E for a receiver at $(10, 0, 1.5)$ m, and (b): E for a receiver at (10, 25, 1.5) m. The frequency discretisations considered are $\Delta_f = 1$ Hz in *solid-black*, $\Delta_f = 0.5$ Hz in *solid-grey*, and $\Delta_f = 0.25$ Hz in *dashed-black*.

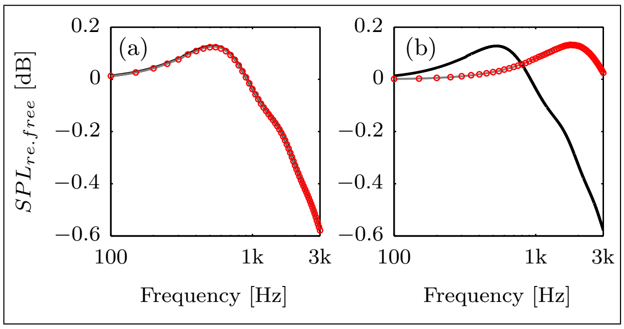

Figure 3. Sound pressure level relative to free field [dB]. (a): $SPL_{re.free}$ for a receiver at $(5, 0, 0)$ m, and (b): $SPL_{re.free}$ for a receiver at (5, 25, 0) m. In addition, we distinguish the 2.5D BEM in *solid grey*, the 2.5D MST in *red circles*, and the 2D MST in *solid black*. In the 2.5D transform we have used $\Delta_f = 0.5$ Hz, and $f_{max} = 3$ kHz

2.3.2. Off-axis scattering by a cylinder

In the next subsection we will consider on-axis and off-axis scattering by a cylindrical object in free-space. The cylinder, with outer radius $r_o = 0.05$ m, is positioned at $(x, z) = (0, 0)$, a monopole source at $(x_s, y_s, z_s) = (-2.5, 0, 0)$, and two receivers at $(x_r, y_r, z_r) = (5, 0, 0)$ and $(x_r, y_r, z_r) = (5, 25, 0)$. In Fig. 3 the sound pressure level relative to free-field ($SPL_{re.free}$) is compared using 2.5D BEM, 2.5D MST, and 2D MST. The latter is only added for comparison reasons. It can be seen that the agreement between the 2.5D MST and 2.5D BEM is good for both cases. Although the difference between the 2.5D methods and the 2D MST for on-axis insonification is hardly visible, it does exist and manifests itself as a very small level offset. For the off-axis case we observe a shift of the complete spectrum to higher frequencies in a similar fashion as discussed in e.g. [5].

3. RESULTS

In the following section the 2.5D MST is used to study sound propagation through arrays of cylinders parallel to the ground. We will use the array cross-sections as shown in Fig. 4 a–c, which have been taken from [13]. In that paper, the authors presented an optimisation procedure to maximise the 2D insertion loss of graded index sonic crystals (GRIN SC) by: (i) organising cylinders in complex formations, and (ii) introduction of line defects. The optimised structures (we use the one depicted in Fig. 4 a) were then compared against: (i) a structure for which the filling fraction was set to the maximum value as shown in Fig. 4 b, and (ii) a square reference structure with line defects as shown in Fig. 4 c. In the following, we refer to structures A, B, and C, for the structures depicted in Fig. 4 a–c, respectively. Note that all structures are 1.2 m tall, are organised in square lattice with lattice constant $a = 0.1$ m, and have a maximum unit-cell filling fraction $ff_{max} = 0.4$. More details about the optimisation procedure and 2D calculation results can be found in [13]. Next, we will investigate the insertion loss (IL) of these structures for off-axis placed monopoles, finite incoherent line sources, and infinite incoherent line sources.

The complex pressure due to a monopole can be found through Eq. 4, whereas the pressure due to a finite incoherent line source is obtained by energetic summation of a series of monopoles distributed along a common line parallel to the y-axis. In case of an infinite incoherent line source the mean square pressure along the y-axis is invariant and may be obtained by [6]:

$$\tilde{p}^2(x,z,k) = \frac{1}{2\pi}\int_{-\infty}^{\infty}\left|q\left(x,z,\sqrt{k^2-k_y^2}\right)\right|^2 dk_y. \quad (11)$$

Let us now investigate the insertion loss (IL) due to a monopole as function of source receiver angle ϕ, which is defined in the $x-y$ plane. The source is assumed to be located at $(x_s, y_s, z_s) = (-2.5, 0, 0.01)$, whereas the receiver is placed at (20, y_r, 1.5), with y_r defined through ϕ. Letting, $\phi = 0$, 37.5, and 75°, gives $y_r = 0$, 17.3, and 84 m, respectively. Insertion losses as function of ϕ are shown in Fig. 4: d–f, and correspond to structures $A-C$, respectively. It can be seen that by increasing ϕ the characteristic response shifts up in frequency for all studied cases. This phenomenon has been previously reported for oblique incident plane waves impinging on infinitely long tube bundles [5], and is sometimes referred to as a *projection effect*. The whole (insertion loss) spectrum for acoustically rigid scatterers shifts approximately according to $f(\phi) \approx f/\cos\phi$. As such, one can get an estimate of the insertion loss spectra for 2.5D geometries without implementing the actual 2.5D transform.

The insertion losses of structures $A-C$ insonified by an infinite incoherent line source are presented in Fig. 4:g. It can be seen that the frequency response looks much different from those presented in Fig. 4:d–f, as rapid oscillations are suppressed due to spectral smearing. Furthermore, we may observe that all

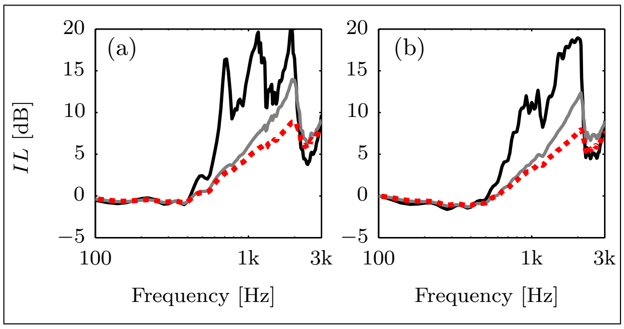

Figure 5. Insertion loss [dB] for finite incoherent line sources of various lengths. The receiver is placed in the centre of the finite incoherent line source at (20, 0, 1.5) m. (a): IL for structure A, (b): IL for structure B. In addition, we distinguish the $\phi = 37.5°$ in *solid, black*, $\phi = 75°$ in *solid, grey*, and $\phi = 90°$ in *dashed, red.*

studied structures exhibit an IL increase between 250 — 2000 kHz, whereas the onset of noise reduction depends on the specific structure. The pass-band at around 2.5 kHz (for on-axis insonification) manifests itself as a dip in the spectrum, but it is clearly less pronounced than in 2D.

The insertion loss spectra as shown in Fig. 4:g correspond to a rather extreme case of an infinite road. More realistically, we assume that the barrier remains infinite, whereas the line source is considered to be finite in length and incoherent. Such a source can be modelled by a series of uncorrelated monopoles, distributed along a common line parallel to the y-axis. With a fine enough source separation dy_s, i.e. the geometrical spacing between the individual monopoles, this can be modelled accurately. When a receiver is positioned in the centre of the finite line source only one half of the source needs to be modelled. As such we distribute a series of monopole sources between $0.5dy_s$ and $y_s = \tan\phi \times |x_s - x_r|$, with $dy_s = 1$ m. Insertion loss spectra of the structures A and B, insonified by a finite incoherent line source as obtained by setting $\phi = 37.5$, 75, and 90°, are presented in Fig. 5. It can be seen that a distinct pass-stop pattern remains for the shortest finite line source studied. However, further increasing the length of the line source results in convergence towards an infinite incoherent line source, as one would expect.

4. Discussion and Conclusions

To study sound propagation through arrays of cylinders parallel to rigid ground the two-and-a-half-dimensional multiple scattering theory (2.5D MST) has been introduced. The proposed method was numerically validated for: (i) a point source above rigid ground, and (ii) off-axis scattering by a cylinder in free-field. For both cases the 2.5D MST was shown to be in excellent agreement with the respective reference method, provided that the frequency resolution

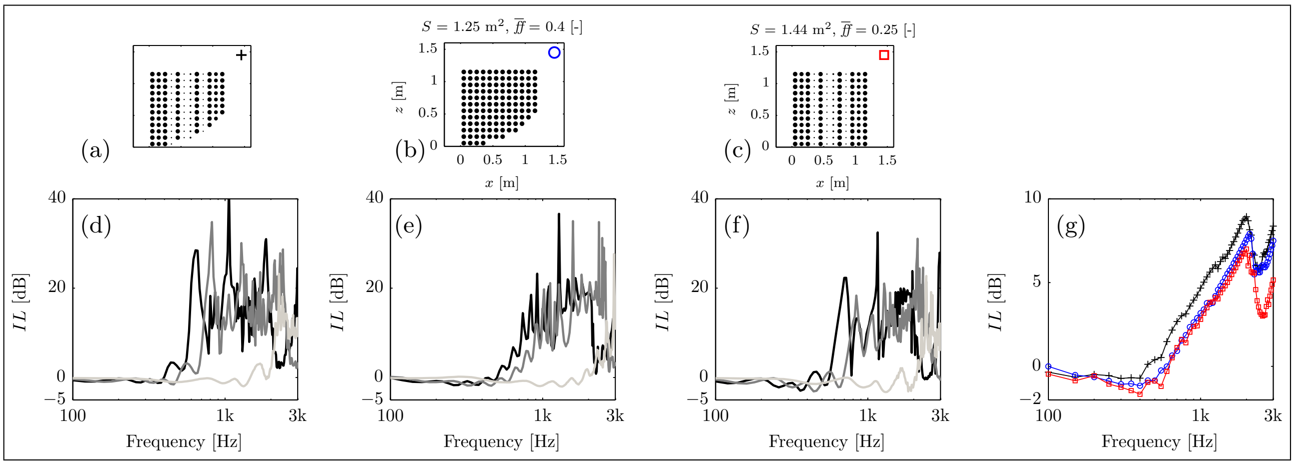

Figure 4. (a – c): Illustration of structures A (left), B (middle), and C (right), and (d – f): narrowband IL [dB] as function of source-receiver angle ϕ. We can distinguish: $\phi = 0°$ in *black*, $\phi = 37.5°$ in *dark grey*, and $\phi = 75°$ in *light grey*. (g): Narrowband IL [dB] for an infinite incoherent line source and a receiver at (20, 0, 1.5) m. We have: structure A in *black crosses*, B in *blue circles*, and C in *red squares*.

of the numerical integration procedure was chosen fine enough. Further, it has been shown that off-axis insonifaction of an array of cylinders parallel to rigid ground will shift the characteristic response to higher frequencies, which is due to a projection effect which has been reported earlier in [5]. In addition, we studied incoherent line sources of finite or infinite length, and found that both these source types introduce a spectral smearing effect. In conclusion, it has been shown that the modelled source type has a strong influence on the noise reducing performance of these structures, and certainly has to be considered when noise control of surface transport noise is of interest.

Acknowledgement

The research leading to these results has received funding from the Swedish Governmental Agency for Innovation Systems - VINNOVA - through the national project Urban Acoustic Screens.

References

[1] L. Zigoneanu, B.-I. Popa, and S. A. Cummer, "Three-dimensional broadband omnidirectional acoustic ground cloak," *Nature Materials*, Mar. 2014.

[2] A. Khelif, A. Choujaa, B. Djafari-Rouhani, M. Wilm, S. Ballandras, and V. Laude, "Trapping and guiding of acoustic waves by defect modes in a full-band-gap ultrasonic crystal," *Physical Review B*, vol. 68, Dec. 2003.

[3] F. Cervera, L. Sanchis, J. Sánchez-Pérez, R. Martínez-Sala, C. Rubio, F. Meseguer, C. López, D. Caballero, and J. Sánchez-Dehesa, "Refractive acoustic devices for airborne sound," *Physical Review Letters*, vol. 88, Dec. 2001.

[4] J. V. Sanchez-Perez, C. Rubio, R. Martinez-Sala, R. Sanchez-Grandia, and V. Gomez, "Acoustic barriers based on periodic arrays of scatterers," *Applied Physics Letters*, vol. 81, no. 27, p. 5240, 2002.

[5] M. A. Heckl, "Oblique sound transmission through tube bundles and tube gratings," *Ultrasonics*, vol. 32, no. 4, pp. 275–286, 1994.

[6] D. Duhamel, "Efficient calculation of the three-dimensional sound pressure field around a noise barrier," *Journal of sound and vibration*, vol. 197, no. 5, pp. 547–571, 1996.

[7] E. M. Salomons, A. C. Geerlings, and D. Duhamel, "Comparison of a ray model and a fourier-boundary element method for traffic noise situations with multiple diffractions and reflections," *Acta Acustica united with Acustica*, vol. 83, no. 1, pp. 35–47, 1997.

[8] P. Jean, J. Defrance, and Y. Gabillet, "The importance of source type on the assessment of noise barriers," *Journal of Sound and Vibration*, vol. 226, no. 2, pp. 201–216, 1999.

[9] M. Hornikx and J. Forssén, "The 2.5-dimensional equivalent sources method for directly exposed and shielded urban canyons," *The Journal of the Acoustical Society of America*, vol. 122, no. 5, p. 2532, 2007.

[10] Y.-Y. Chen and Z. Ye, "Acoustic attenuation by two-dimensional arrays of rigid cylinders," *Physical Review Letters*, vol. 87, 2001.

[11] L. Sanchis, F. Cervera, J. Sánchez-Dehesa, J. V. Sánchez-Pérez, C. Rubio, and R. Martínez-Sala, "Reflectance properties of two-dimensional sonic band-gap crystals," *Journal of the Acoustical Society of America*, vol. 109, no. 6, p. 2598, 2001.

[12] B. van der Aa and J. Forssén, "Shape-optimal design of graded index sonic crystal formations using natural cubic splines," *Applied Acoustics*, vol. 78, pp. 98–111, Apr. 2014.

[13] B. van der Aa and J. Forssén, "Shape-optimal design of graded index sonic crystal noise barriers with line defects," (Internoise, Innsbruck), 2013.